

Self-organizing timing allocation mechanism in distributed wireless sensor networks

Hisa-Aki Tanaka¹, Hiroya Nakao², and Kenta Shinohara¹

¹ Department of Electric Engineering, The University of Electro-Communications
1–5–1 Chofugaoka, Chofu-shi 182–8585, Japan

² Department of Physics, Kyoto University, Kyoto 606–8502, Japan

Abstract: A novel, distributed timing allocation method [2, 3, 4, 5] has been proposed for packet collision avoidance in wireless sensor networks recently. In this paper, this proposed method is theoretically examined, and a hidden self-organization mechanism is unveiled. As the result, some important fundamental questions regarding this method are reasonably resolved. Namely, our present analysis provides a definite criterion, as to when it functions properly for densely connected networks in real noisy environments.

Keywords: nonlinear dynamics, self-organization, wireless sensor network

Classification: Science and engineering for electronics

References

- [1] D. Estrin, R. Govindan, J. Heidemann, and S. Kumar, “Next Century Challenges: Scalable Coordination in Sensor Networks,” *ACM Mobicom Conf.*, Seattle, WA, Aug. 1999.
- [2] H. Tanaka, talk at symposium session in 2003 autumn meeting of physical society of Japan. PPT slides are available at [Online] <http://synchro3.ee.uec.ac.jp/literature/butsuri20030922.pdf>
- [3] M. Date, H. Tanaka, and Y. Morita, Japanese patent number 417389, 19th Sept. 2003 (filing date). Summary is available at [Online] <http://www.j-tokkyo.com/2005/H04L/JP2005-094663.shtml>
- [4] Y. Kubo and K. Sekiyama, “Communication Timing Control with Interference Detection for Wireless Sensor Networks,” *EURASIP Journal on Wireless Communications and Networking*, vol. 2007, 2007.
- [5] Summary is available at [Online] http://www.soumu.go.jp/main_sosiki/joho_tsusin/scope/event/h20yokousyu/session1/network3.pdf
- [6] Y. Kuramoto, *Chemical Oscillations, Waves, and Turbulence*, Berlin, Germany: Springer, 1984; Lecture Notes in Physics, vol. 39, 1975.
- [7] K. Okuda, “Variety and generality of clustering in globally coupled oscillators,” *Physica D*, vol. 63, pp. 424–436, 1993.

1 Introduction and motivation of the study

Wireless sensor networks (WSNs) [1] are now utilized for a variety of distributed sensing purposes; indoor, outdoor, mobile commerce and even in-body monitoring applications. They are usually made up with wireless sensor nodes; small, cheap, and resource limited devices sensing the environment and communicating with each other. In such WSNs, one of the challenging and important design principles is the idea of scalability, which means that the function of WSNs should not be influenced when the number of sensor nodes is arbitrarily varied even time-dependently. Therefore, communication protocols for WSNs generally require distributed, adaptive, and even a self-organizing mechanism.

As mentioned above, each sensor node (SN) is generally resource limited, so each SN usually shares a common communication band with other SNs. This means that if multiple communications take place simultaneously in a WSN, they interfere with each other, and, in the worst case, data packets collide with each other and can be lost in the network. Hence, for WSNs, it is essential to avoid collisions of data packets in advance.

Two major approaches have been developed for collision avoidance in WSNs: carrier sense multiple access with collision avoidance (CSMA/CA) and (distributed versions of) time division multiple access (TDMA). However, neither of these methods is perfect for the following reasons. Namely, CSMA/CA requires that the density of SNs is relatively low and the traffic is not so heavy. Also, TDMA requires global timing synchronization of all SNs, as well as computation and communication overheads in each SN, to allocate the communication timings in advance.

Motivated by the above mentioned situation, an alternative collision avoiding method has been proposed recently [2, 3], which is expected to meet the need for more flexible techniques with less communication overheads. The original idea of this method comes from a certain self-organizing mechanism of timing allocation process, which will be analyzed in this paper. Improvements of this method have been continued for these several years [4, 5]. However, we have not been able to explain why this method generates the correct timing allocations for SNs clearly. This paper reveals the hidden mechanism behind the presented method [2, 3, 4, 5], and explains why this method functions properly, for the first time. Also, some new findings are provided, which are useful for further applications of this method.

2 Framework of the distributed timing allocation method

In this paper, we consider a simple, realistic situation of a WSN with N sensor nodes (SNs) being located in a single small room, as shown in Fig. 1 (a). Here, each SN can communicate with all other SNs, as its range of wireless communication is supposed to be several tens of meters. Namely, in this particular example, the network has a densely connected topology. It should be emphasized that such densely connected (sub)networks are often embedded in a widely distributed multi-hop network. Therefore, the following analy-

sis of the densely connected network provides an essential building block for understanding more general, widely distributed networks.

Here, we assume that each SN periodically transmits a timing beacon (and a data packet if it has any sensing data at this stage) to other SNs, which can be a short pulse whose timing information is expressed as the timing of transmission in itself. Also, we denote the period of transmissions as T . Since each SN communicates periodically, it is convenient to introduce a phase variable $\phi(t)$ ($\in [0, 2\pi]$) for each SN. Then, for the i th SN in the network, we can identify its instantaneous timer value as $\phi_i(t)$, and it is naturally assumed that $\phi_i(t)$ increases as $\phi_i(t) = \frac{2\pi}{T}t + \phi_i(0)$. Namely, the instantaneous state of each SN is mapped to a rotating phase point ‘o’ on the circle as shown in Fig. 1 (b) or 1 (c). In addition, we assume that each SN transmits a timing beacon (and a data packet) when its $\phi_i(t)$ value becomes 0. From this coordination of $\phi(t)$, it is now clear that a reasonable allocation of transmission timings for N SNs can be either a uniformly distributed pattern of Fig. 1 (b), or an evenly clustered pattern of Fig. 1 (c), because each SN is able to avoid packet collisions by using such allocated timings, which is similar to the ones in TDMA. One simple way for obtaining such timing allocations is given as follows. For each ϕ_i that evolves according to $\frac{d\phi_i}{dt} = \frac{2\pi}{T} (\equiv \omega)$, we introduce mutual interactions between the i th and j th SNs. Since this interaction between i th and j th SNs is uniquely coordinated by the phase difference of $\phi_i - \phi_j$, we assume that the interaction is expressed by a function $\Gamma(\phi_i - \phi_j)$ as shown in Fig. 1 (d). Then, one possible modeling of the timing allocation process can be given as

$$\frac{d}{dt}\phi_i(t) = \omega + \frac{1}{N} \sum_{j=1}^N \Gamma(\phi_i - \phi_j) + \sqrt{2D}\xi_i(t), \quad (i = 1, \dots, N), \quad (1)$$

where Γ is the 2π -periodic function of $\phi_i - \phi_j$, and ξ_i is the external noise whose intensity is given by the parameter D ($D = 0$ for the noiseless case). See [2, 3, 4] for more detailed and extensive descriptions of this modelling. In Eq. (1), $1/N$ is a normalization factor, which is necessary in taking the large N limit properly. We note that the functions Γ in Fig. 1 (d) have a ‘repulsive’ effect on any pair of i th and j th SNs. Namely, each pair of SNs tends to avoid having similar values of $\phi_i(t)$ and $\phi_j(t)$ at any moment, which is nothing but the collision avoidance.

This idea and its simulation results were presented at [2], and then soon later applied for the patent of [3]. Since then, its improvements and further applications have been presented (see [4], for example), and even experimental verifications have been recently conducted in real environments [5]. For all these progresses, the very essential questions have remained to be unsolved, which are listed as follows. (i) How does the allocation process of Eq. (1) lead to reasonable patterns such as in Fig. 1 (b) or Fig. 1 (c)? (ii) How can we choose the function Γ so as to obtain the specific pattern of Fig. 1 (b) or Fig. 1 (c)? (iii) To what extent is the presented method robust to the external noises $\xi_i(t)$?

It should be emphasized that these questions are important, as they represent the unknown self-organizing mechanism of the presented method.

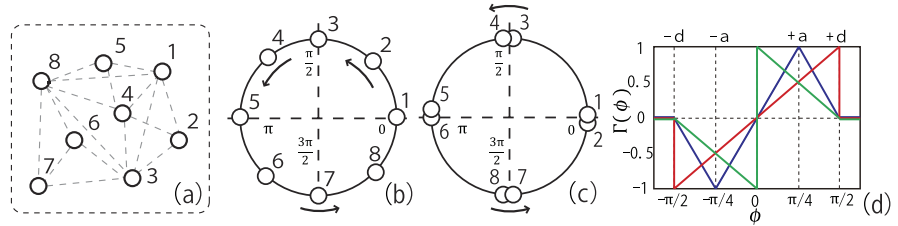


Fig. 1. (a) Sensor networks of N nodes ($N = 8$, for instance). (b), (c) Resulting timing allocation for type1 and type2 functions, and (d) Function Γ with a tuning parameter a (blue line); type1 function (green line, $a = 0$), type2 function (red line, $a = d$).

3 Systematic simulations and analysis

To answer these questions systematically, we introduce the following family of the function Γ ,

$$\Gamma(\phi) = -\frac{\phi + d}{d - a} \quad (-d \leq \phi < -a), \quad \frac{\phi}{a} \quad (|\phi| \leq a), \quad -\frac{\phi - d}{d - a} \quad (a < \phi \leq d), \quad (2)$$

and $\Gamma(\phi) = 0$ for $d < |\phi| < \pi$, as shown in the graph in Fig. 1(d), and consider the effect of external noise by tuning a and D . The constant d ($0 \leq d \leq \pi$) in Eq. (2) determines the range of phase interaction for each SN, and the parameter a ($0 \leq a \leq d$) tunes the shape of Γ . Then, this family of the function Γ includes both the type1 and type2 functions as the $a \rightarrow 0$ and $a \rightarrow d$ limits, respectively, as in Fig. 1(d). Note that these two specific functions have already been considered in [4] and in [2, 3], respectively.

First, we present results of systematic simulations for timing allocations from Eq. (1). Without loss of generality, we can put $\omega = 0$ in Eq. (1) by moving to a rotating frame and redefining the phase variables as $\phi_i + \omega t \rightarrow \phi_i$ for all i . In addition to direct simulations of Eq. (1) for finite N , we also perform numerical simulations of the corresponding nonlinear Fokker-Planck equation [6],

$$\frac{\partial}{\partial t} P(\phi, t) = -\frac{\partial}{\partial \phi} \left\{ \left[\int_0^{2\pi} \Gamma(\phi - \theta) P(\theta, t) d\theta \right] P(\phi, t) \right\} + D \frac{\partial^2}{\partial \phi^2} P(\phi, t), \quad (3)$$

which can be derived from Eq. (1) in the $N \rightarrow \infty$ limit. This describes the dynamics of the one-body probability density function (PDF) $P(\phi, t)$ of the phase ϕ of any oscillator at time t , and this $P(\phi, t)$ indicates how the allocated timings $\phi_i(t)$ are distributed on the circle of $[0, 2\pi]$ in the $N \rightarrow \infty$ limit. Thus, $P(\phi, t)$ is 2π -periodic in ϕ as $P(\phi + 2\pi, t) = P(\phi, t)$ and normalized as $\int_0^{2\pi} P(\phi, t) d\phi = 1$. Note that Eq. (3) always has a uniform stationary solution, $P_0(\phi) = 1/2\pi$, corresponding to the uniform state. However it may

be unstable and cannot be observed in some situations, reflecting non-trivial dynamics of Eq. (1). Here, we also note that Eq. (1) has been analyzed and phase clustering behavior due to certain repulsive interactions have been demonstrated in [7]. However, [7] focuses on the noiseless situation, whereas our present analysis is for real environments with noises and for distinct class of phase coupling functions with extremely simple functional forms.

In the following simulations, we fix the constant d as $\pi/2$ for instance, and vary the parameter a . Figure 2 (a) shows typical snapshots of the phase variables for the type1 ($a = 0$) and type2 ($a = \pi/2$) functions obtained by direct numerical simulations of Eq. (1) with $N = 500$ and $D = 0.01$ of small noise, starting from random initial conditions. The resulting phase variables ϕ_i ($i = 1, \dots, 500$) at $t = 100$ are almost uniformly spread in $[0, 2\pi]$ for the type1 function (black crosses), whereas they are split into several groups (4 clusters in this example) for the type2 function (red circles). Figure 2 (b) compares normalized phase histograms obtained from Eq. (1) with the stationary PDFs from Eq. (3) for several values of a , showing good agreement. The phase is uniformly distributed over $[0, 2\pi]$ for relatively small values of a (e.g. $a = 0$, black crosses in Fig. 2 (b)), whereas they exhibit regularly aligned peaks for larger values of a (e.g. $a = 1.2$ and $\frac{\pi}{2}$, blue circles and red triangles, respectively in Fig. 2(b)), reflecting the formation of phase clusters. Thus, the system undergoes a transition from the uniform state of $P_0(\phi) = 1/2\pi$ to clustered states as the parameter a is increased.

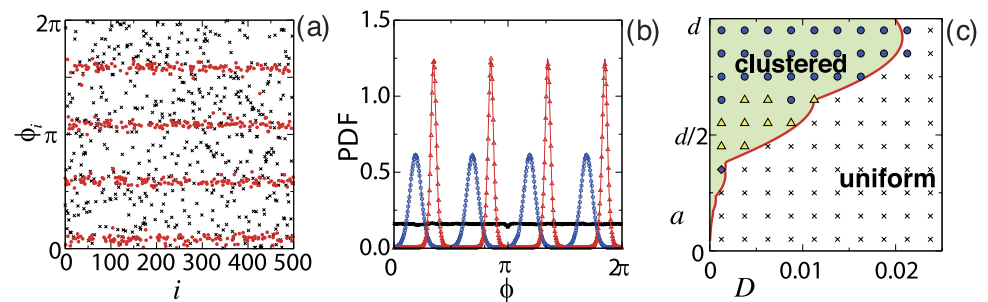


Fig. 2. (a) Typical snapshot of phase variables ϕ_i from Eq. (1) for the type1 and type2 functions. (b) Normalized histograms and PDFs of ϕ . Data points and curves are respectively obtained from Eq. (1) and Eq. (3), showing a good match. (c) Stability diagram of the uniform state and observed patterns.

To understand this observed transition, we perform a linear stability analysis of the uniform state by applying a small perturbation $q(\phi, t)$ to the uniform solution $P_0(\phi) = 1/2\pi$ and examining whether this perturbation decays or not. Substituting $P(\phi, t) = P_0(\phi) + q(\phi, t)$ into Eq. (3), a linearized equation of $q(\phi, t)$ is easily obtained. Expanding $q(\phi, t)$ and $\Gamma(\phi)$ into Fourier series as $q(\phi, t) = \sum_{m=-\infty}^{\infty} e^{im\phi} q_m(t)$ and $\Gamma(\phi) = \sum_{m=-\infty}^{\infty} e^{im\phi} \Gamma_m$ with $q_m(t)$ and Γ_m being Fourier coefficients, this linearized equation of $q(\phi, t)$ is decom-

posed into linear equations of the form $\dot{q}_m(t) = (-im\Gamma_m - Dm^2)q_m(t)$ for $m = -\infty, \dots, +\infty$. Thus, for each q_m , the real part of the linear growth rate λ_m is given by $\lambda_m = m\Gamma_m^{(I)} - Dm^2$ where $\Gamma_m^{(I)}$ is the imaginary part of Γ_m . The uniform solution $P_0(\phi)$ is linearly stable if λ_m is negative for all m (except λ_0 that is constantly zero). If λ_m is positive at some values of m , the uniform solution is destabilized and the corresponding Fourier modes grow.

By calculating Γ_m from Eq. (2), the growth rate λ_m is explicitly obtained,

$$\lambda_m = \frac{d}{\pi(d-a)} \left(\frac{\sin md}{md} - \frac{\sin ma}{ma} \right) - Dm^2 \quad (m = -\infty, \dots, \infty). \quad (4)$$

Then, in the type1 limit ($a \rightarrow 0$), we obtain $\lambda_m = -\frac{1}{\pi} \left(1 - \frac{\sin md}{md} \right) - Dm^2$. Clearly, λ_m is always negative for any m (except λ_0 being 0), so the uniform state is stable. On the contrary, in the type2 limit ($a \rightarrow d$), $\lambda_m = \frac{1}{\pi} \left(\cos md - \frac{\sin md}{md} \right) - Dm^2$ is obtained, which becomes positive when m is near $2\pi/d$ and its integer multiples, for small D . Therefore, the uniform state does become unstable and the clustered states may possibly be organized. In between these two limits, there exists a critical value of a at a_c , where the uniform state changes its stability. Note that the noise always tends to stabilize the uniform state, and, if D is sufficiently large, no mode of m becomes unstable even in the type2 limit. Therefore, a critical value D_c of the noise intensity D also exists.

Figure 2(c) shows a stability diagram of the uniform state, together with the observed stationary patterns from direct numerical simulations of Eq. (1). The red thick curve represents the set of critical parameter pairs (a_c, D_c) where the uniform state changes its stability. Note that this curve is obtained from the condition that $\lambda_m = 0$ for all m , and in the upper region (colored in green) of this curve, $\lambda_m > 0$ is always satisfied for some m . Also, the result of direct simulations of Eq. (1) for $N = 100$ nodes is plotted on each grid in Fig. 2(c). Filled marks with color indicate phase-clustered states (\circ in blue: 4-cluster, Δ in yellow: 5-cluster, and \diamond in violet: 9-cluster) and crosses (\times in black) indicate the uniform state. We see that cluster states are actually formed in this region of a and D where λ_m is positive and the uniform state is unstable (slight discrepancy is due to finite-size effect).

The above facts reveal the self-organizing mechanism behind the presented method, so reasonable answers are thus provided for the three basic questions posed in the chapter 2.

4 Conclusions

In this paper, we have revealed the self-organizing mechanism in the timing allocation method [2, 3, 4, 5] for densely connected WSNs. Theoretical and partly numerical results obtained here provide useful guidelines leading to proper functioning of the proposed method. More specifically, to the question (i) posed in the end of chapter 2, the linear stability and the associated mode analysis of Eq. (3) provides reasonable understanding of this mechanism. Also, to the question (ii) and (iii), the theoretically obtained criterion shown

in Fig. 2 (c) gives a useful information, which is expected to provide further application of the proposed method.

In addition to such practical significance of the result, the analysis here sheds a new light on the uncovered side of synchronization phenomena, long forgotten since [7]. Further analysis and experiments are expected to explore this new area of researches in distributed systems.